Nuclear Physics B154 (1979) 283–300

HEAVY QUARKONIA AND ASYMPTOTIC FREEDOM

Hartmut KRASEMANN
II. Institut für Theoretische Physik der Universität Hamburg, Germany

Seiji ONO *
Institut für Theoretische Physik der RWTH Aachen, Germany

Received 26 February 1979

We use semiclassical methods to discuss the scaling behaviour of quarkonium level splittings up to $M(Q\bar{Q}) = 200$ GeV. Special emphasis is laid on the effects of asymptotic freedom which are found to be essential for $M(Q\bar{Q}) \gtrsim 30$ GeV. The bound $t\bar{t}$ system will almost look like the Υ system except that $R = \Delta M(^3P_2 - {}^3P_1)/\Delta M(^3P_1 - {}^3P_0)$ is larger than 0.8. In the Υ system R will already be close to 0.8.

1. Introduction

Since the discovery of the first quarkonium system, namely the charmonium states J/ψ and ψ' in November 1974, these new states have been welcome as a laboratory for asymptotic freedom and quark confinement. Although the first hopes of finding a large variety of perturbative tests of QCD already in the charmonium system were soon destroyed, the observation of the Υ and Υ' resonances in an e^+e^- storage ring (DORIS) ** revived the hope of finding such tests in quarkonia which are heavier and therefore much less relativistic than charmonium. With the present (PETRA) and future machines it may well be that we will find at least one more quarkonium even heavier than Υ, Υ'. Since the complicated nature of the inter-quark forces seems not to allow its understanding with only one "hydrogen atom", these systems are highly welcome. In this paper we investigate the level splittings, fine structure and electronic widths as a function of the quark mass, so that a comparison of different quarkonia may allow one to draw conclusions about the forces between quark and antiquark.

We start with a discussion of a reasonable static potential for quarkonium in sect. 2, which will be inserted in the Schrödinger equation which in turn is solved numerically. All spin effects are treated *via* the Fermi-Breit Hamiltonian. In sect. 3 we

* Supported by the Bundesministerium für Forschung und Technologie.
** For an experimental review of the Υ system, see, e.g., ref. [1].

then try to make some very simple and crude estimates for the scaling behaviour of the 2S – 1S mass differences, the P-wave splittings, the S-wave splittings and the behaviour of $\Gamma_{e\bar{e}}$ of the ground state. These estimates are then checked by detailed numerical calculations in sect. 4. This is done in three different models which all bear the characteristics of asymptotic freedom. For comparison we also study a model with an ordinary Coulomb component in the static potential (which is not asymptotically free). Our conclusions are summarized in sect. 5.

2. The $Q\bar{Q}$ potential

In QCD, the coupling constant $g = (4\pi\alpha_s)^{1/2}$, renormalized at the relevant momentum transfer Q^2 or the corresponding distance R, turns out to be a monotonously falling function of Q^2 (or rising function of R). It tends logarithmically to 0 as $q^2 \to \infty$ or $R \to 0$: asymptotic freedom [2]. This implies that at small distances or large Q^2 the chromomagnetic interaction between quarks becomes very similar to the electromagnetic interaction between electrons, because α_s is small. At short distances the interquark potential is essentially of the Coulomb type,

$$V_{\mathrm{Coul}}(R) = -\frac{4}{3}\frac{\alpha_s(Q_0^2)}{R}, \tag{2.1}$$

where the $\frac{4}{3}$ is a colour group constant. Eq. (2.1) is strictly speaking only an approximation to the interquark potential at the momentum transfer Q_0^2 where $\alpha_s(Q_0^2)$ has been renormalized. Q_0^2 will be different for bound states, whose sizes are different. One can, however, renormalize α_s in X-space so that α_s becomes a function of R rather than Q_0^2 [3]:

$$V_{\mathrm{AF}}(R) = -\frac{4}{3}\frac{\alpha_s(R)}{R} \tag{2.2}$$

is a unique function of R with *

$$\alpha_s(R) = \frac{12\pi}{25}\frac{1}{2\ln(\mu/R)} \tag{2.3}$$

with the renormalisation distance μ. Eq. (2.3) looks very similar to the corresponding formula in momentum space [2],

$$\alpha_s(Q^2) = \frac{12\pi}{25}\frac{1}{\ln(Q^2/\Lambda^2)}. \tag{2.4}$$

In principle μ is calculable from the renormalisation mass $\Lambda = 500$ MeV, as measured in deep inelastic lepton scattering. However, one has to go beyond the leading log

* α_s also depends on the number of effective (light) flavours, 4 for the Υ system and 5 for a 30 GeV $t\bar{t}$ system. We use (2.3) for 4 flavours as an approximation for any quarkonium.

approximation and the calculation becomes very difficult. Celmaster, Georgi and Machacek [4] therefore construct the static short-distance potential between quarks as a Fourier transform of the gluon propagator

$$\alpha_s(q^2)/q^2 \,, \tag{2.5}$$

with $\alpha_s(q^2)$ given by (2.4). They find eqs. (2.2), (2.3) up to terms of the order $\ln^{-3}(1/R)$ and establish a relation between μ and Λ : $\mu = (\Lambda\, e^{\gamma})^{-1}$ with γ = Eulers constant. Since $e^{\gamma} = 1.78$, μ is of the same order of magnitude as Λ^{-1}. We will fix μ to $\mu = 0.5$ fm as suggested from hadron radii, non-perturbative transverse jet momenta and the effective α_s of 0.3 to 0.4 in charmonium analyses *. From (2.3) it is immediately clear that (2.2) is only valid for distances $R \ll \mu$.

For distances $R \gg 0.5$ fm there is another picture which gives us hints about the nature of the $Q\bar{Q}$ potential. For such large distances lattice gauge theories [5] or the string model [6] suggest that the $Q\bar{Q}$ force is completely independent of the interquark distance and the quark spin. It should also be independent of the quark mass and flavour. This gives rise to a universal scalar and linear confinement potential

$$V_{\text{conf}} = aR \,. \tag{2.6}$$

The Regge trajectories of light meson spectra suggest that the interquark force at large distances is $a \simeq 0.7$ ..... 0.8 GeV/fm, when evaluated in BS type models, Schrödinger type models or the string model. We adopt a to be universal, $a = 0.787$ GeV/fm [7].

For distances around 0.5 fm, however, we have no hints how the static potential should look. The QCD coupling α_s is certainly large, so that perturbation theory breaks down. On the other hand, the interquark distance is not yet large compared to the scale parameter μ, i.e., the colour flux string between quark and antiquark is not yet long enough to result in a constant force. We have to guess the form of the $Q\bar{Q}$ potential at these intermediate distances (0.2 to 1 fm roughly) and then check it in the charmonium *and* Υ system.

The intermediate potential has to interpolate between the regions of asymptotic freedom and confinement. One might therefore speculate that the slope and the curvature of this intermediate potential have to decrease faster with R than those of V_{AF} (2.2) and more slowly than those of V_{conf} (2.6).

This condition is certainly fulfilled by the potential of Bhanot and Rudaz [7], although these authors did *not* incorporate asymptotic freedom:

$$V_1(R) = \begin{cases} -\frac{4}{3}\,\alpha_s/R \,, & R < R_1 \,, \\ b \log(R/c) \,, & \text{for } R_1 < R < R_2 \,, \\ aR \,, & R > R_2 \,. \end{cases} \tag{2.7}$$

* We have checked that our results are insensitive to the exact value of μ as can be expected from the logarithmic dependence on μ.

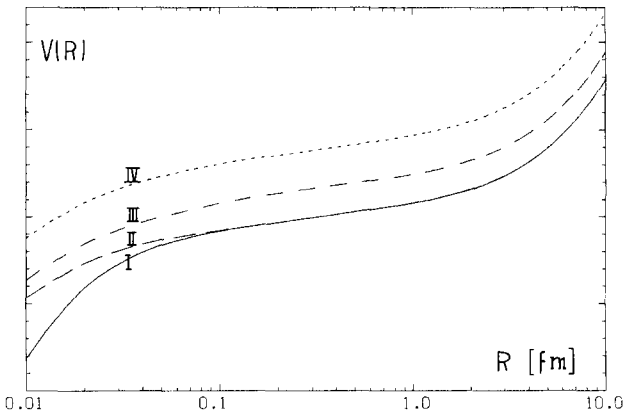

Fig. 1. The potentials I to IV, compare table 1.

R_1, R_2, b and c were uniquely determined from α_s and a by demanding $V(R)$ to be continuously differentiable at R_1 and R_2. The potential (2.7) successfully fits charmonium and it predicted the $\Upsilon' - \Upsilon$ mass difference to be 560 MeV. The fit parameters are an effective α_s of $\alpha_s = 0.31$ and $a = 0.787$ GeV/fm, which coincide with our prejudices about α_s and a. To study the scaling properties of the $Q\bar{Q}$ system and especially the influence of asymptotic freedom as in V_{AF} of eq. (2.2), we use this potential (2.7), referred to as model I, and a variation, referred to as model II, see fig. 1.:

$$V_{II}(R) = \begin{cases} -\frac{8}{25}\pi\,(R\log(\mu/R))^{-1} + c_1\,, & R < R_1\,, \\ b\log(R/c)\,, & \text{for } R_1 < R < R_2\,, \\ aR\,, & R > R_2\,. \end{cases} \tag{2.8}$$

Here b, c, a, R_2 are as in (2.7), $\mu = 0.5$ fm, $R_1 = 0.07192$ fm, and $c_1 = 0.3978$ GeV guarantees that $V(R)$ is smooth at R_1. For comparison we also study two potentials, referred to as model III and IV, of the form

$$V_{III,\,IV}(R) = V_{AF}(R) + V_{int}(R) + a \cdot R\,, \tag{2.9}$$

where $V_{AF}(R)$ is given by (2.2), (2.3) for $R < \mu/\exp(1)$ and set to be constant for larger values of R. V_{int} has the form (i = III, IV) (compare table 1):

$$V_{int}(R) = -b_i \exp(-R/c_i)\,. \tag{2.10}$$

V_{int} is of limited variation and is similar to the potential used by Celmaster, Georgi and Machacek [4]. It is unimportant compared to V_{AF} at small distances and zero at large distances. We have also tried a potential of the form (2.9) with

$$V_{int}(R) = b\log(R/c)\,, \tag{2.11}$$

but find no parameters b, c to describe charmonium with it. The reason is that

Table 1
The four potentials investigated

Model	m_c (GeV)	$V(R)$		Parameters [a]
I [b]	1.05	$V(R) = \begin{cases} -(4/3)\,\alpha_s/R \\ b\,\log(R/c) \\ aR \end{cases}$	for $R < R_1$ for $R_1 \leqslant R \leqslant R_2$ for $R > R_2$	$\alpha_s = 0.31$, $c = (4\alpha_s/3a)^{1/2}$, $b = c\,a\exp(1)$, $R_1 = c\exp(-1)$, $R_2 = c\exp(1)$.
II	1.05	$V(R) = \begin{cases} -8\pi(25R\log(\mu/R))^{-1} + c_1 \\ b\,\log(R/c) \\ aR \end{cases}$	for $R < R_1$ for $R_1 \leqslant R \leqslant R_2$ for $R > R_2$	$c_1 = 0.3978$ GeV, $R_1 = 0.07192$ fm, c, b, R_2 as in model I.
III	1.05	$V(R) = V_{AF}(R) - b\exp(-R/c) + aR$		$b = 1.394$ GeV, $c = 0.185$ fm.
IV	1.95	$V_{AF}(R) = \frac{-8\pi}{25} \times \begin{cases} (R\log(\mu/R))^{-1} \\ \exp(1)/\mu \end{cases}$	for $R < \mu\exp(-1)$ for $R \geqslant \mu\exp(-1)$	$b = 1.219$ GeV, $c = 0.250$ fm.

Compare also fig. 1. For the choice of parameters see text.
[a] In all models $a = 0.787$ GeV/fm, $\mu = 0.5$ fm
[b] Ref. [7].

$\log(R)$ is too far-reaching and interferes with the $a \cdot R$ part in the confinement regime $R > 1$ fm.

The quark mass is a relatively unrestricted parameter for light quarkonia, say below 10 GeV, where $M_V \sim 2m_Q$ needs not hold. This is demonstrated by various reasonable fits to charmonium with m_c between 1 and 2 GeV [8]. The reason is that quantities like $\Gamma_{e\bar{e}}(\psi')/\Gamma_{e\bar{e}}(J/\psi)$, which safely can be used in lowest-order formulae, are insensitive to m_c. They essentially allow one to fix the shape of the potential only. The experimentally known quantities most sensitive to m_c are the absolute values of $\Gamma_{e\bar{e}}(J/\psi)$ and $\Gamma_{e\bar{e}}(\psi')$. But at this point theoretical ambiguities enter. QCD knows a very large first-order (α_s) correction to the Schrödinger wave function of $c\bar{c}$ at the origin [9]

$$|R(0)|^2_{1^{st}\text{order}} = |R(0)|^2_{\text{Schröd}} \left(1 - \frac{16\alpha_s}{3\pi}\right), \tag{2.12}$$

which has to be inserted into the formula for the leptonic width [10]

$$\Gamma_{e\bar{e}}(V) = \alpha^2 e_Q^2 |R(0)|^2 (\tfrac{1}{2}M_V)^{-2} . \tag{2.13}$$

Because of the large correction, (2.12), the first as well as the zeroth-order formula for $\Gamma_{e\bar{e}}$ seems unreliable, and so does any determination of m_c *via* (2.13). Consequently we study models with two extreme values for m_c. In models I to III, m_c = 1.05 GeV, as can be found from (2.13) with $|R(0)|^2$ in zeroth order. In model IV, m_c = 1.95 GeV, as is consistent with (2.13) including the first-order correction, (2.12).

We discuss S- and P-wave splittings in terms of the Fermi-Breit Hamiltonian:

$$H^{LS} = A\, \boldsymbol{L} \cdot \boldsymbol{S} \equiv (A' - C)\, \boldsymbol{L} \cdot \boldsymbol{S}\,, \quad H^{T} = B(3\boldsymbol{\sigma}_1 \cdot \hat{\boldsymbol{R}}\boldsymbol{\sigma}_2 \cdot \hat{\boldsymbol{R}} - \boldsymbol{\sigma}_1\boldsymbol{\sigma}_2)\,, \quad H^{ss} = D\boldsymbol{\sigma}_1 \cdot \boldsymbol{\sigma}_2$$

$$A' = \frac{3}{2m_Q^2}\frac{1}{R} d_R V_{\text{spin}}(R)\,, \qquad C = \frac{-1}{2m_Q^2}\frac{1}{R} d_R(aR)\,, \tag{2.14}$$

$$B = \frac{-1}{12m_Q^2}\left(d_R^2 - \frac{1}{R} d_R\right) V_{\text{spin}}(R)\,, \quad D = \frac{1}{6m_Q^2}\Delta V_{\text{spin}}(R)\,,$$

where the spin dependence of the potential is

$$\Gamma^\mu V \Gamma^\mu = \gamma^\mu V_{\text{spin}} \gamma^\mu + \mathbb{1}\, V_{\text{conf}}\, \mathbb{1}\,, \tag{2.15}$$

with $V_{\text{spin}}(R) = V(R) - aR$. We neglect all spin-independent corrections in the Fermi-Breit Hamiltonian, since their net effect is small.

3. Scaling estimates by hand

Before we turn to numerical calculations in sect. 4 we want to get a feeling for the aspects of scaling by a very crude but simple calculation [11]. For this purpose

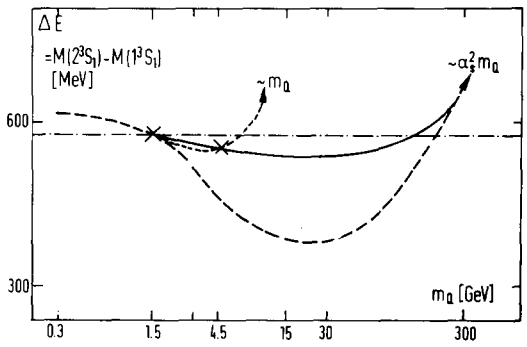

Fig. 2. Estimates of the scaling behaviour of $\Delta E(Q\bar{Q})$ in: dashed curve, the "standard potential" according to eqs. (3.4), (3.5); dotted curves, the "standard potential" with α_s = const; dot-dashed curve, the logarithmic potential; full curve, this is our final hand-made guess.

we take the "standard potential"

$$V(R) = -\tfrac{4}{3}\,\alpha_s/R + aR\,, \tag{3.1}$$

with the Coulomb part as a small spin-dependent perturbation to the spin-independent linear potential aR. We further use the scaling laws of E and R in a linear potential

$$E \sim R \sim m_Q^{-1/3}\,. \tag{3.2}$$

This gives us for the potential (3.1)

$$E \sim m_Q^{-1/3} + \epsilon' \langle -\tfrac{4}{3}\,\alpha_s/R \rangle\,, \tag{3.3}$$

and for the *difference* of energies 2S − 1S

$$\Delta E(2S - 1S) \sim m_Q^{-1/3} + \epsilon\alpha_s(m_Q)\, m_Q^{1/3}\,. \tag{3.4}$$

Fixing the constant ϵ in the charmonium system now allows to estimate ΔE for heavier quarkonia. The m_Q dependence of α_s is taken into account *via* eq. (2.4). For $m_Q \gtrsim 100$ GeV this perturbative ansatz breaks down: the Coulomb potential dominates. Here we have

$$\Delta E \sim \alpha_s^2(m_Q)\, m_Q \sim m_Q \log^{-2}(m_Q\mu)\,. \tag{3.5}$$

We thus ((3.4) and (3.5)) obtain the dashed line in fig. 2. The decrease of ΔE up to $m_Q \simeq 30$ GeV is consistent with earlier numerical calculations by Eichten and Gottfried [12]. If one keeps α_s constant as m_Q varies, the Coulomb singularity shows up much earlier, as is also indicated in fig. 2 (dotted line). The $\Upsilon' - \Upsilon$ mass difference suggests that the potential at intermediate distances is somewhat similar to a log potential, in which ΔE = const. Such a logarithmic component added to $V(R)$ in (3.1) would tend to fill up the valley of the dashed curve for ΔE in fig. 2. Our hand-

made final guess for the scaling behaviour of $\Delta E(2^3S_1 - 1^3S_1)$ is shown as solid line in fig. 2.

We now estimate perturbative splittings within the standard potential (3.1). From there and (2.14) we have

$$H^T, H^{LS}_{spin} \sim \frac{1}{m_Q^2}\left\langle \frac{1}{R} d_R \frac{-\alpha_S}{R} \right\rangle \sim \frac{\alpha_S}{m_Q^2 R^3} \sim \frac{\alpha_S}{m_Q}, \tag{3.6}$$

where $H^{LS}_{spin} = A' \boldsymbol{L} \cdot \boldsymbol{S}$ is that part of H^{LS} arising from V_{spin} alone. The last relation in (3.6) holds as long as the wave functions are governed by the linear potential. The spin-independent (confinement) part of the potential, however, contributes to the Thomas precession, $H^{LS}_{conf} = C \boldsymbol{L} \cdot \boldsymbol{S}$ (compare (2.14))

$$H^{LS}_{conf.} \sim \frac{1}{m_Q^2}\left\langle \frac{1}{R} d_R(aR) \right\rangle \sim \frac{a}{m_Q^2 R} \sim \frac{a}{m_Q^{5/3}}. \tag{3.7}$$

Using experimental masses as input we can fix A and B for charmonium *:

$$A_P = 34 \text{ MeV}, \qquad B_P = 10 \text{ MeV}, \qquad \text{in } c\bar{c}\,\text{P waves}. \tag{3.8}$$

A, B and C can now be estimated for heavy quarkonia using (3.8) as input and (3.6), (3,7) as the scaling laws. For $m_Q > 100$ GeV the wave function will become more and more Coulombic, so that asymptoticcally H^T, $H^{LS}_{spin} \sim \alpha_S m_Q$ and $H^{LS}_{conf} \sim 1/m_Q$. This estimate is displayed in fig. 3.

An interesting ratio is

$$R_P = \frac{M(^3P_2) - M(^3P_1)}{M(^3P_1) - M(^3P_0)} = \frac{2A - \frac{12}{5}B}{A + 6B}. \tag{3.9}$$

The expected scaling behaviour of R_P *via* eq. (3.6) and (3.7) is also shown in fig. 3. It is clear that, asymptotically, $R \to 0.8$.

The spin-spin splittings are determined through parameter D of eq. (2.14). In the standard model D is a point-like operator since $\Delta(-1/R) = 4\pi\,\delta^{(3)}(R)$

$$D = \frac{1}{6m_Q^2} \langle \Delta V_{spin}(R) \rangle = \frac{2}{9}\frac{\alpha_S}{m_Q^2} |R(0)|^2. \tag{3.10}$$

D therefore scales as $R^{-3} m_Q^{-2}$. It is very hard to evaluate the scaling behaviour of D without detailed calculations, since the wave function at the origin is sensitive to the Coulomb singularity. With the wave functions of a pure linear potential $D \sim m_Q^{-1}$, this is a clear underestimate. With Coulomb wavefunctions $D \sim m_Q$, this is a clear overestimate. The truth lies in between. But asymptotically the wave functions become Coulombic, and D is given by the Coulomb wave function at the origin

$$D \sim \alpha_s^4(m_Q)\, m_Q \sim m_Q \log^{-4}(m_Q \mu). \tag{3.11}$$

* In the standard potential $A' = 6B$, so that $C = 6B - A = 26$ MeV in charmonium. Thus the Thomas precession is very important for the magnitude of the P-wave splittings.

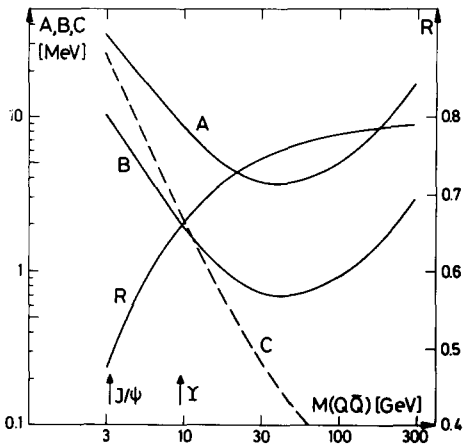

Fig. 3. Estimates of the parameters A, B, C and the ratio R_P of (3.9) as a function of m_Q according to (3.6), (3.7) with charmonium (3.8) as input.

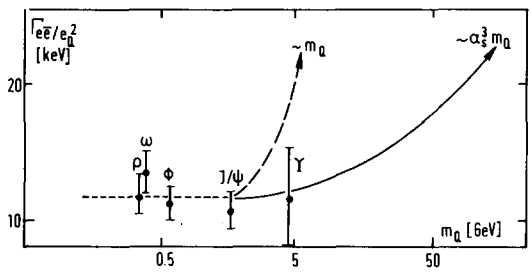

Fig. 4. Estimates of the scaling behaviour of $\Gamma_{e\bar{e}}/e_Q^2$: dotted curve, experimental evidence below $m_Q = 5$ GeV; dahes curve, in a pure Coulomb potential; full curve, in the asymptotically free one-gluon exchange potential according to (3.12).

Relating D to the leptonic width *via* (2.13) we find for $\Gamma_{e\bar{e}}$ in asymptopia

$$\Gamma_{e\bar{e}}(V) \sim \alpha_s^3 m_Q \sim m_Q \log^{-3}(m_Q \mu) \,. \tag{3.12}$$

This can be understood as an upper bound for the whole m_Q regime and is displayed in fig. 4.

4. Model calculations

We begin with a discussion of model I which has an ordinary Coulomb singularity at the origin and model II, where this singularity is weakened by asymptotic freedom.

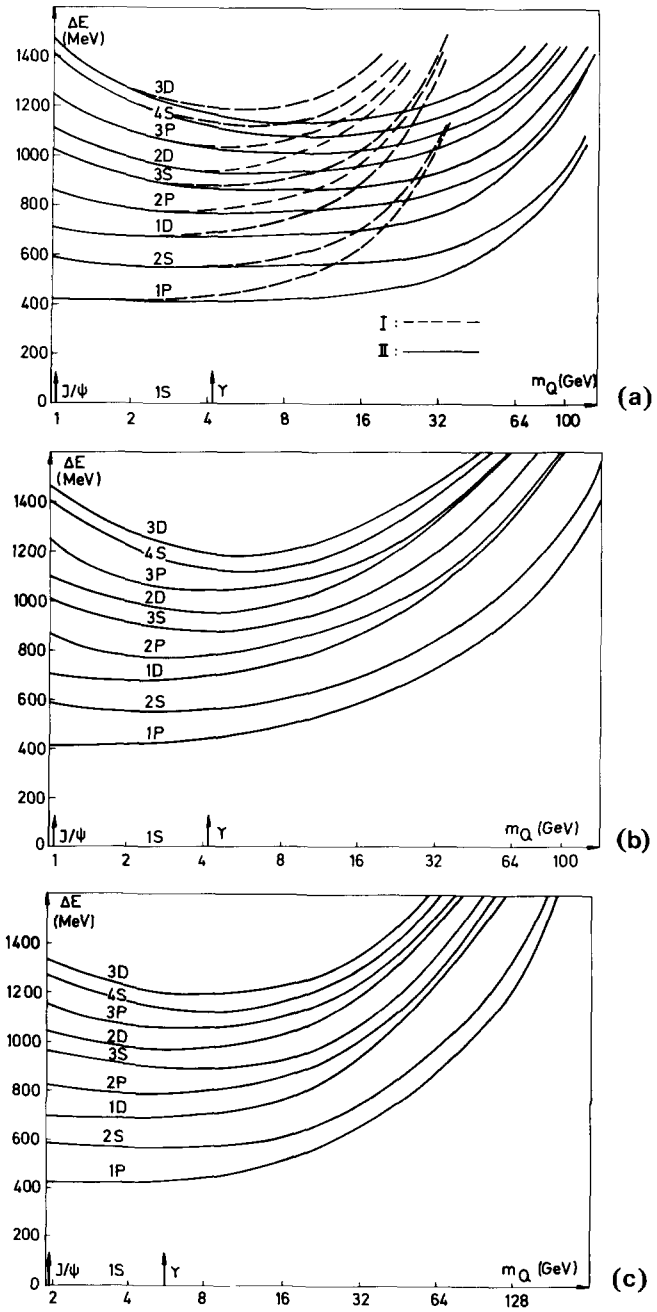

Fig. 5. Mass differences of the first S-, P- and D-wave excitations to the ground state in (a) models I and II, (b) model III and (c) model IV.

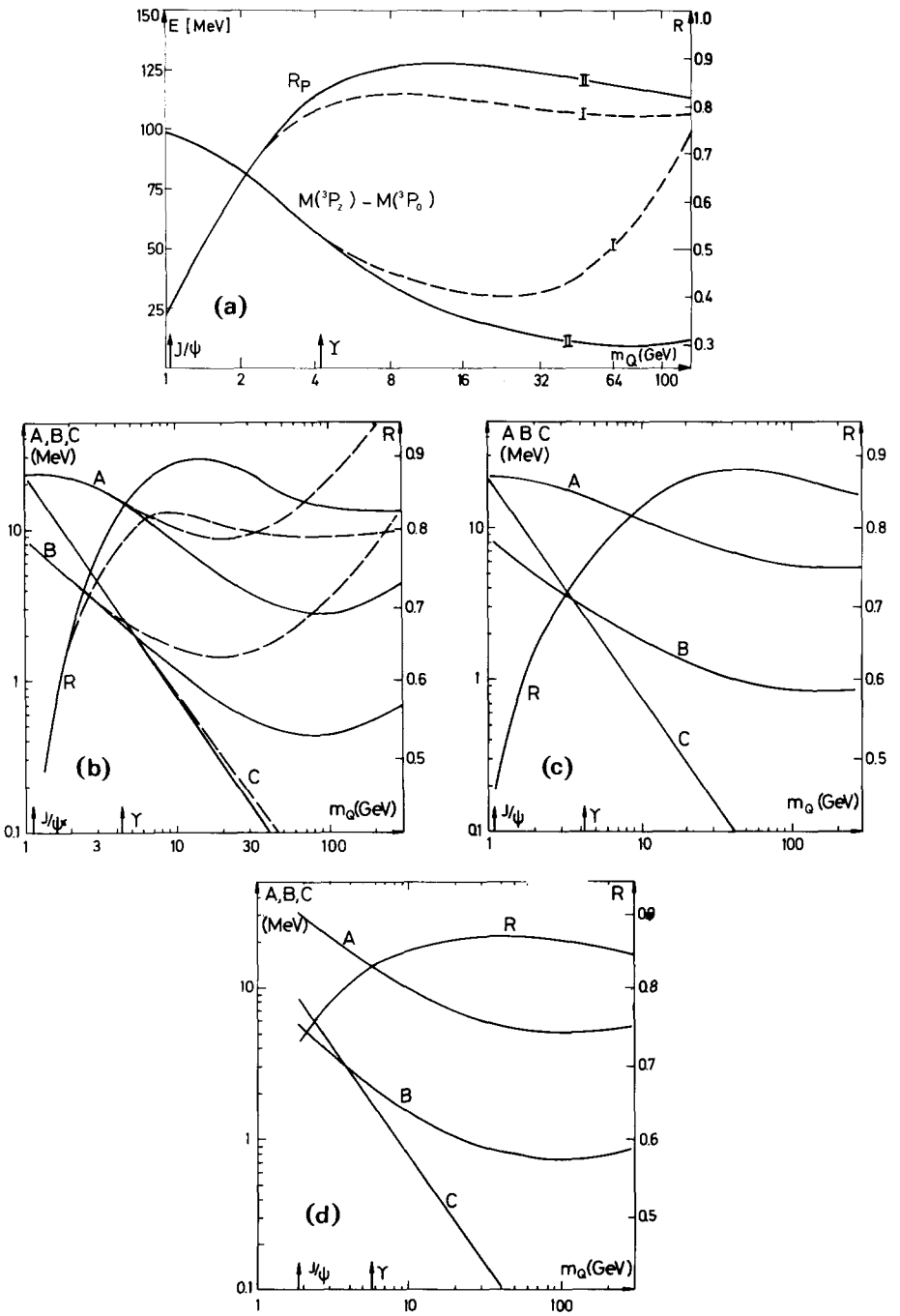

Fig. 6. Spin-orbit splitting of P-waves as a function of m_Q. (a) The mass difference $\Delta M(^3P_2 - {}^3P_0)$ and the ratio R of (3.9) in models I and II. (b) to (d) The parameters A, B and C as defined by (2.14) in all models. R is given for the models III and IV. (b) shows models I (dashed curve) and model II, (c) shows model III and (d) model IV.

All our potentials are displayed in fig. 1. We have calculated the mass differences between the first few S-, P- and D-waves and display these with respect to the ground state mass in fig. 5a. The influence of the stronger singularity of model I is clearly seen. In model II the logs associated with the coupling strength of the one gluon exchange weaken this singularity substantially: for $m_Q \lesssim 15$ GeV the level differences to the ground state remain essentially the same as in the Υ system. For $m_Q > 15$ GeV they increase only very slightly. To demonstrate that this effect is really due to the form of the short-range potential (2.2) and rather independent of the special ansatz for the intermediate potential or the choice of m_c and m_b we investigate the potentials V_{III} and V_{IV}, see (2.9), (2.10) and the table 1.

The mass differences in these models are shown in fig. 5b and c, respectively. In both cases we find that the level differences again increase much more slowly than in model I. This slow down of the increase of ΔE with m_Q is due to the functional form of the short-range QCD potential (2.2), (2.3), i.e., to asymptotic freedom. For quark masses larger than 30 GeV the special choice of the intermediate potential (between 0.1 and 1 fm) becomes irrelevant, because the Bohr radius of the system becomes smaller than 0.1 fm.

We now turn to perturbative spin-orbit splittings of P- and D-waves. We have calculated the parameters A, B, C as explained by (2.14) in all four models assuming (2.15). In fig. 6a we show the absolute P-wave splitting $M(^3P_2) - M(^3P_0)$ together with the ratio R_P of (3.9) as a function of m_Q in models I, II. Figs. 6b to d show the parameters A, B, C and R in all models.

From fig. 6 one reads off that in all four models the ratio R_P of eq. (3.9) increases fast from charmonium to the Υ system, where it is almost 0.8. For 5 GeV $\leqslant m_Q \leqslant$ 30 GeV the value of R is influenced by the intermediate part of the potential whose details are unknown in principle. But for $m_Q \geqslant 30$ GeV also the intermediate part of the potential becomes unimportant and we can state a clear difference between model I and models II–IV. In model I, R approaches its asymptotic value of 0.8 from below. In models II–IV, however, R approaches the asymptotic value of 0.8 from above. This is a direct consequence of the asymptotically free one-gluon exchange. The short-range QCD forces decrease slower with the distance than Coulomb forces. Therefore R has to be larger than 0.8!

We found an interesting effect for the D-wave splittings in charmonium, which led us to plot (for D-waves) the parameters A and B, which are defined by eq. (2.14), as well as the ratio R,

$$R_D = \frac{M(^3D_3) - M(^3D_2)}{M(^3D_2) - M(^3D_1)} = \frac{3A_D - \frac{18}{7}B_D}{2A_D + 4B_D}, \tag{4.1}$$

in fig. 7. The four models differ in m_c (m_c = 1.05 GeV in I, II, III and 1.95 GeV in IV). This leads to substantially different Thomas precession contributions from the confinement potential. While for m_c = 1.95 GeV the charmonium D-multiplet is normal ordered, it is inverted for m_c = 1.05 GeV. The reason is obvious: for a smaller m_c the wave functions reach out farther in space and feel substantially more of the

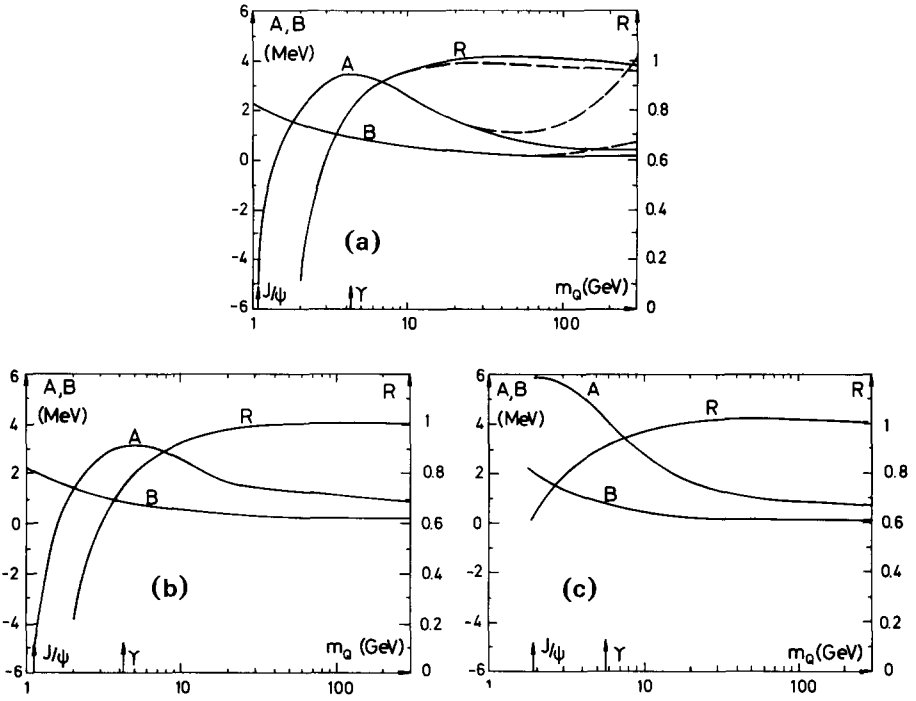

Fig. 7. Spin-orbit splitting of D-waves as a function of m_Q in (a) models I (dashed curve) and II, (b) model III and (c) model IV. We also give R for the D-waves as defined by (4.1). The parameters A and B are again defined by (2.14).

confinement forces. A measurement of any other charmonium D-wave than the $^3D_1 = \psi''$ (3.77) might be able to restrict the dynamical charmed quark mass much more than other experimental input.

The behaviour of the D-wave splittings at high quark masses is already familiar from the behaviour of the P-wave splittings. Also here R_D approaches the asymptotic value of $\frac{27}{28}$ from above.

We continue by considering spin-spin splittings and $\Gamma_{e\bar{e}}$, both quantities which supposedly are only sensitive to the wave function at very short distances. While due to the lack of trustworthy experimental candidates for pseudoscalar quarkonium states * the computed spin-spin splittings cannot reliably be compared to experiment, $\Gamma_{e\bar{e}}$ usually is the first known quantity of a quarkonium state, when produced in e^+e^-. We will therefore discuss only one quarkonium decay: $\Gamma_{e\bar{e}}$. However, one should remember the large ambiguities in $\Gamma_{e\bar{e}}$ introduced through the large first-order correction to the Schrödinger wave function at the origin, as given by (2.12). In

* The possible candidates suffer from the fact that one cannot explain the magnetic dipole transitions to and from these states.

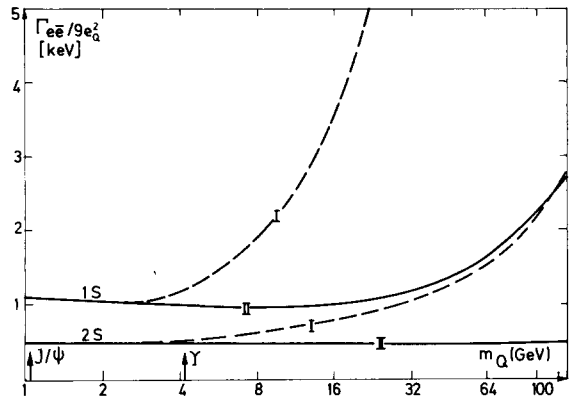
$\Gamma_{e\bar{e}}/9e_Q^2$ [keV]
1S
2S
I
II
J/ψ
ϒ
m_Q (GeV)

(a)

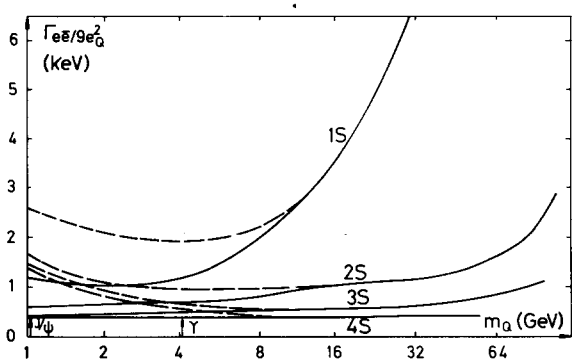
$\Gamma_{e\bar{e}}/9e_Q^2$ (keV)
1S
2S
3S
4S
J/ψ
ϒ
m_Q (GeV)

(b)

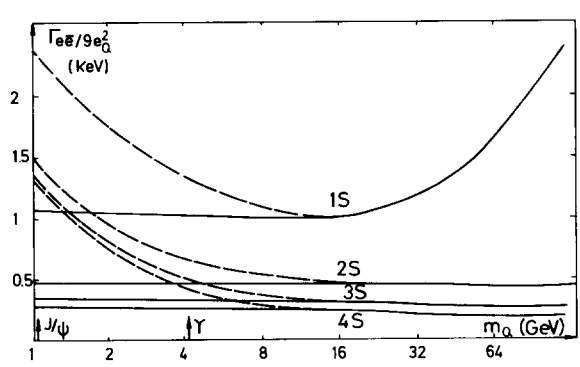
$\Gamma_{e\bar{e}}/9e_Q^2$ (KeV)
1S
2S
3S
4S
J/ψ
ϒ
m_Q (GeV)

(c)

Fig. 8.

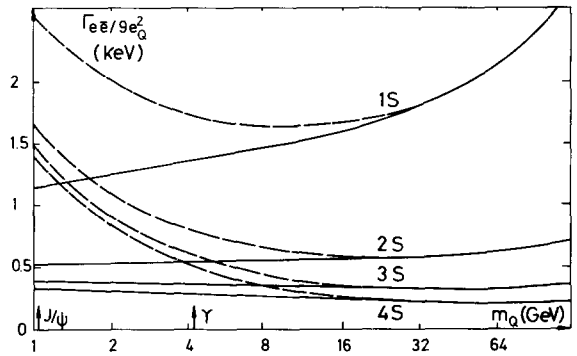

(d)

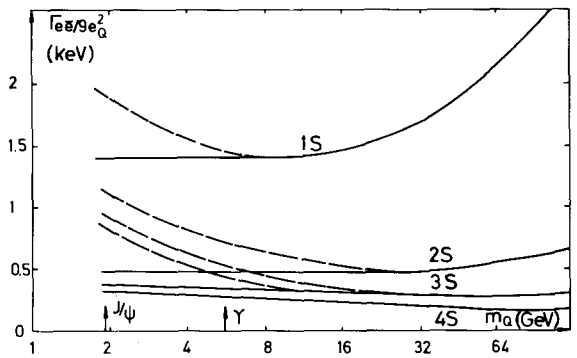

(e)

Fig. 8. $\Gamma_{e\bar{e}}/9e_Q^2$ as a function of m_Q in all models. (a) A comparison of model I and II for the two lowest S-waves, (b) to (e) For the first four S-waves in models I (b), II (c), III (d) and IV (e). The dashed lines give $\Gamma_{e\bar{e}}(M_V/2m_Q)^2/9e_Q^2$, a quantity proportional to $|\psi(0)|^2/m_Q^2$. For large m_Q we have set $M_V = 2\,m_Q$. In models I to III eq. (2.13) has been taken literally, while in model IV the correction (2.12) is applied.

order to cover a wide range of possible procedures, we take formula (2.13) literally for models I, II, III and include the first-order (α_s) correction in model IV. For very heavy quarkonia this makes no difference anyway. $\Gamma_{e\bar{e}}(m_Q)$ is plotted in fig. 8.

The spin-spin splittings are governed by H^{ss} in eq. (2.14). While in model I $\Delta V_{spin}(R)$ essentially results in a δ-function, this is no longer true if one has the logarithmic weakening of the Coulomb singularity through asymptotic freedom as in models II to IV. Here the Laplacian of V_{spin} is a regular function and the matrix elements of H^{ss} have to be computed using the wave functions of quarkonium states. For S-waves the spin-spin splittings in models II to IV are considerably smaller than in model I. This is understood as an effect of the overestimate of $|\psi(0)|^2$ in

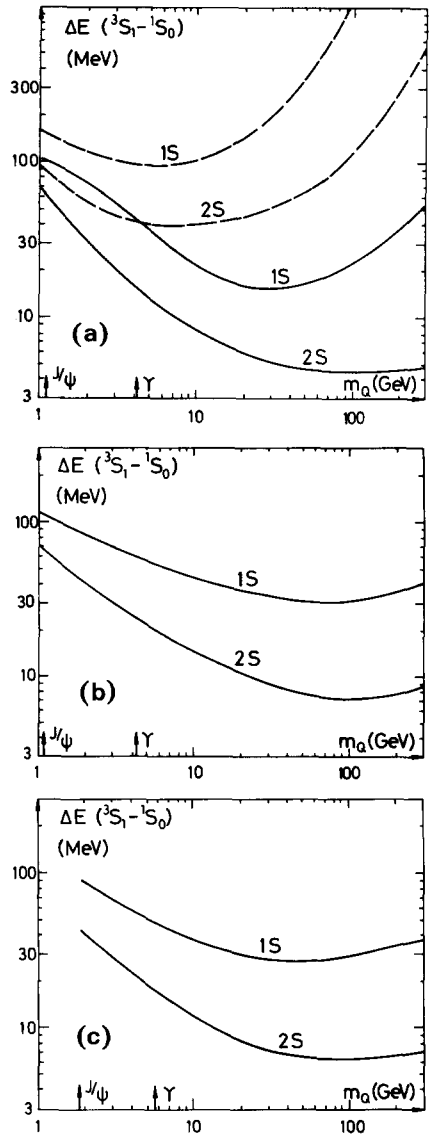

Fig. 9. The hyperfine splittings of quarkonium as a function of m_Q in (a) model I (dashed curve) and model II; (b) model III; (c) model IV.

model I because of the too strong Coulomb singularity. The effective smearing of $|\psi(0)|^2$ and the weaker singularity of $V_{\text{spin}}(R)$ lead to the smaller spin-spin splittings in models II to IV; compare fig. 9.

The scaling behaviour of $\Gamma_{e\bar{e}}$ and H^{ss} gives no surprise, it follows the same trends

as that of H^{LS}, H^{T} and the gross splittings. It is noteworthy, however, that the quantity most sensitive to asymptotic-freedom corrections is $\Gamma_{e\bar{e}}$ of the quarkonium ground state. Without asymptotic freedom it would double between $m_Q = 5$ GeV and $m_Q = 15$ GeV while the asymptotic-freedom nature of the one-gluon exchange potential guarantees that $\Gamma_{e\bar{e}}$ does not double before $m_Q \gtrsim 70$ GeV!

5. Conclusions

We have calculated the level splittings and the fine structure for quarkonia between 3 and 200 GeV. We find that in a potential model without asymptotic freedom (model I) the Coulomb singularity of the one-gluon exchange becomes manifest for $m_Q > 8$ GeV. The wave function of the ground state at the origin increases rapidly for $m_Q > 8$ GeV. At the same time the level splittings to the ground state start to increase, but a bit more slowly. At $m_Q = 15$ GeV the mass difference $2S - 1S = 700$ MeV, but $\Gamma_{e\bar{e}}$ has already doubled compared to $m_Q = 5$ GeV. If we compare model I to models II, III, IV, which *include* the effects of asymptotic freedom (especially model II differs from model I only in this respect), there is no difference for m_Q below 5 GeV. The present quarkonia, charmonium and the Υ system, do not allow to test the idea of asymptotic freedom! But above $m_Q = 5$ GeV without asymptotic freedom the ground state becomes Coulombic very soon, this is not the case in all three different models which incorporate asymptotic freedom. The logs in the short-range one-gluon exchange potential lead to a scaling behaviour of all quantities which is very similar to that in an overall $\log(R)$ potential for a wide m_Q regime between 2 and 30 GeV. At the same time these logs are responsible for the fact that $R_P = \Delta M(^3P_2 - {}^3P_1)/\Delta M(^3P_1 - {}^3P_0)$ becomes larger than 0.8: the short-range QCD potential is softer than the Coulomb potential. If quarkonia have something to do with QCD and asymptotic freedom, then the next quarkonium will at first sight look the same as the Υ system! Only for m_Q larger than 30 GeV can the slow inset of the weakened singularity in the short-distance potential be observed. For $m_Q \simeq 100$ GeV, $\Gamma_{e\bar{e}}$ will almost have doubled for the ground state. Also the $2S - 1S$ mass difference will almost have doubled by then. The fine and hyperfine splittings will still be considerably below their magnitudes in charmonium, and the spectrum in general will be much more Coulombic.

We can summarize that, although the similarity of the Υ spectrum with charmonium is hardly related to asymptotic freedom, exactly this asymptotic-freedom feature of the one-gluon exchange is responsible for the fact that the next quarkonia up to 60 GeV will at first sight again look the same as the Υ or charmonium system except for $R_P > 0.8$. For the Υ P-waves, R_P will be close to 0.8.

We thank T.F. Walsh for a helpful discussion on the manuscript. H.K. thanks the theory group at the RWTH Aachen for its hospitality. S.O. thanks P.M. Zerwas for his encouragement.

References

[1] G. Flügge, Tokyo Conf. 1978, DESY 78/55.
[2] D.J. Gross and F. Wilczek, Phys. Rev. Lett. 30 (1973) 1343;
H.D. Politzer, Phys. Rev. Lett. 30 (1973) (1346).
[3] V.B. Berestetski, Sov. Phys. Usp. 19 (1976) 934.
[4] W. Celmaster, H. Georgi and M. Machacek, Phys. Rev. D17 (1978) 879.
[5] K.G. Wilson, Phys. Rev. D10 (1974) 2445;
J. Kogut and L. Susskind, Phys. Rev. D11 (1975) 395.
[6] H. Nielsen and P. Olesen, Nucl. Phys. B61 (1973) 45;
J. Kogut and L. Susskind, Phys. Rev. D9 (1973) 2273;
Y. Nambu, Phys. Rev. D10 (1974) 4262;
B. Brout, F. Englert and W. Fischler, Phys. Rev. Lett. 36 (1975) 649.
[7] G. Bhanot and S. Rudaz, Phys. Lett. 78B (1978) 119.
[8] A. Billoire and A. Morel, Nucl. Phys. B135 (1978) 131.
[9] R. Barbieri, G. Gatto, R. Kögerler and Z. Kunszt, Phys. Lett. 57B (1975) 455.
[10] H. Pietschmann and W. Thirring, Phys. Lett. 21 (1966) 713;
R. van Royen and V.F. Weisskopf, Nuovo Cim. 50 (1967) 617; 51 (1967) 583.
[11] M. Krammer and H. Krasemann, Quarkonium, Karlsruhe lecture 1978, DESY 78/66.
[12] E. Eichten and K. Gottfried, Phys. Lett. 66B (1977) 286.